Parson, W. W. (1987) in *New Comprehensive Biochemistry: Photosynthesis* (Amesz, J., Ed.) pp 43-62, Elsevier, Amsterdam.
Plijter, J. J., Aalbers, S. E., Barends, J. P. F., Vos, M. H., & Van Gorkom, H. J. (1988) *Biochim. Biophys. Acta 935*, 299-306.
Powles, S. B. (1984) *Annu. Rev. Plant Physiol. 35*, 15-44.
Rutherford, A. W. (1986) *Biochem. Soc. Trans. 14*, 15-17.
Rutherford, A. W. (1989) *TIBS 14*, 227-232.
Sandusky, P. O., & Yocum, C. F. (1988) *Biochim. Biophys. Acta 936*, 149-156.
Sétif, P., & Mathis, P. (1980) *Arch. Biochem. Biophys. 204*, 477-485.
Styring, S., Virgin, I., Ehrenberg, A., & Andersson, B. (1990) *Biochim. Biophys. Acta 1015*, 269-278.
Takahashi, Y., Hansson, Ö., Mathis, P., & Satoh, K. (1987) *Biochim. Biophys. Acta 893*, 49-59.
Theg, S. M., Jursinic, P. A., & Homann, P. H. (1984) *Biochim. Biophys. Acta 766*, 636-646.
Theg, S. M., Filar, L. J., & Dilley, R. A. (1986) *Biochim. Biophys. Acta 849*, 104-111.
Thompson, L. K., & Brudvig, G. W. (1988) *Biochemistry 27*, 6653-6658.
Towbin, H., Staehelin, T., & Gordon, J. (1979) *Proc. Natl. Acad. Sci. U.S.A. 76*, 4350-4354.
Trebst, A. (1986) *Z. Naturforsch. 41C*, 240-245.
Trebst, A., Depka, B., & Kipper, M. (1990) in *Current Research in Photosynthesis* (Baltscheffsky, M., Ed.) Vol. I, pp 217-223, Kluwer Academic Publishers, Dordrecht.
Vass, I., Mohanty, N., & Demeter, S. (1988) *Z. Naturforsch. 43C*, 871-876.
Vermaas, W. F. J., Rutherford, A. W., & Hansson, Ö. (1988) *Proc. Natl. Acad. Sci. U.S.A. 85*, 8477-8481.
Virgin, I., Styring, S., & Andersson, B. (1988) *FEBS Lett. 233*, 408-412.
Virgin, I., Hundal, T., Styring, S., & Andersson, B. (1990) in *Current Research in Photosynthesis* (Baltscheffsky, M., Ed.) Vol. II, pp 423-426, Kluwer Academic Publishers, Dordrecht.
Wang, W. Q., Chapman, D. J., & Barber, J. (1990) in *Current Research in Photosynthesis* (Baltscheffsky, M., Ed.) Vol. II, pp 515-518, Kluwer Academic Publishers, Dordrecht.
Yerkes, C. T., & Babcock, G. T. (1980) *Biochim. Biophys. Acta 590*, 360-372.
Yerkes, C. T., Kramer, D. M., Fenton, J. M., & Crofts, A. R. (1990) in *Current Research in Photosynthesis* (Baltscheffsky, M., Ed.) Vol. II, pp 381-384, Kluwer Academic Publishers, Dordrecht.

Kinetic Analysis of Cooperative Interactions Induced by Mn^{2+} Binding to the Chloroplast H^+-ATPase†

R. Hiller and C. Carmeli*
Department of Biochemistry, Tel Aviv University, Tel Aviv 69978, Israel
Received January 30, 1989; Revised Manuscript Received January 8, 1990

ABSTRACT: The kinetics of Mn^{2+} binding to three cooperatively interacting sites in chloroplast H^+-ATPase (CF_1) were measured by EPR following rapid mixing of the enzyme with $MnCl_2$ with a time resolution of 8 ms. Mixing of the enzyme-bound Mn^{2+} with $MgCl_2$ gave a measure of the rate of exchange. The data could be best fitted to a kinetic model assuming three sequential, positively cooperative binding sites. (1) In the latent CF_1, the binding to all three sites had a similar on-rate constants of $(1.1 \pm 0.04) \times 10^4$ M^{-1} s^{-1}. (2) Site segregation was found in the release of ions with off-rate constants of 0.69 ± 0.04 s^{-1} for the first two and 0.055 ± 0.003 s^{-1} for the third. (3) Addition of one ADP per CF_1 caused a decrease in the off-rate constants to 0.31 ± 0.02 and 0.033 ± 0.008 s^{-1} for the first two and the third sites, respectively. (4) Heat activation of CF_1 increased the on-rate constant to $(4.2 \pm 0.92) \times 10^4$ M^{-1} s^{-1} and the off-rate constants of the first two and the third site to 1.34 ± 0.08 and 0.16 ± 0.07 s^{-1}, respectively. (5) The calculated thermodynamic dissociation constants were similar to those previously obtained from equilibrium binding studies. These findings were correlated to the rate constants obtained from studies of the catalysis and regulation of the H^+-ATPase. The data support the suggestion that regulation induces sequential progress of catalysis through the three active sites of the enzyme.

The H^+-ATPase from chloroplasts utilizes an electrochemical potential of protons for the synthesis of ATP from ADP and P_i (McCarty & Carmeli, 1982). Its catalytic sector (CF_1)[1] is a complex having a subunit stoichiometry of 3α, 3β, γ, δ, and ϵ (Morony et al., 1983). Subunit interaction is a major regulatory process in the function of the H^+-ATPase of chloroplasts as it is in similar enzymes from other sources such as mitochondria and bacteria. Negative cooperativity in nucleotide binding is accompanied with a faster catalysis (Cross, 1981), while positive cooperativity in the binding of divalent metal ions is accompanied with a slow down in pre-steady-state catalysis (Carmeli et al., 1981). In accordance with earlier proposals, Stroop and Boyer (1987) suggested that equivalent interactions of the three catalytic β subunits occur as they

† This work was supported by grants from BSF/87 to C.C. and from the U.S. Department of Energy (DE-FG03-88ER 13845) to P. D. Boyer.
* Address correspondence to this author.

[1] Abbreviations: Hepes, *N*-(2-hydroxyethyl)piperazine-*N*′-2-ethanesulfonic acid; CF_1, coupling factor 1 of chloroplast H^+-ATPase; EBT, Eriochrome black T.

0006-2960/90/0429-6186$02.50/0

participate in sequential order of catalysis.

In studies reported here, quantitative evaluation of the cooperativity of Mn^{2+} binding was studied by measurements of binding and release of Mn^{2+} from CF_1. MnATP, like MgATP, serves as substrate, and free Mn^{2+} has inhibitory effects similar to Mg^{2+}. Therefore, information about Mn^{2+} binding is likely to be applicable to the binding of Mg^{2+} and of the substrate. In previous studies, we have found that CF_1 contains three positively cooperative strong Mn^{2+} binding sites (Hillel et al., 1984; Hiller & Carmeli, 1985; Haddy et al., 1985). These were suggested to be the active sites because covalent modification of an arginine residue by naphthylglyoxal, which inhibits catalysis (Takabe et al., 1982), also inhibits the cooperativity among the Mn^{2+} binding sites. Direct measurements by X-ray absorption (EXAFS) of the metal reveal the existence of ternary complexes of enzyme, Mn^{2+}, and ATP at these sites (Carmeli et al., 1986).

Assuming that the cooperativity interactions among the subunits are related to changes in the binding constants of ligands, the kinetics of ligand binding could be related to the conformational changes. Preliminary measurements of the rate of Mn^{2+} binding to CF_1 supported this assumption (Carmeli et al., 1987). In these experiments, rate constants of slow and medium range (0.05 and 1 s^{-1}, respectively) were found. These correlate to two of the three time scales found in kinetic studies of the H^+-ATPase. The third fast rate constant (50–400 s^{-1}) is typical to the rate of catalysis (Bruist & Hammes, 1982; Junesch & Graberr, 1987). The medium time scale is characteristic of control processes such as the pre-steady-state acceleration of ATPase activity in the absence of divalent metal ions (Carmeli et al., 1981) and of the light-induced activation of ATPase activity in chloroplasts pretreated with thiol reagents (Bakker-Grunwald & Van Dam, 1974). Among the slow processes are the pre-steady-state kinetics of ATPase in the presence of divalent ions (Carmeli et al., 1981), the preillumination time in the presence of thiol reagents required for activation of hydrolytic and synthetic activities in chloroplasts (Bakker-Grunwald & Van Dam, 1974), and the concomitant release of tightly bound ADP (Strotman & Bickel-Sandkotter, 1977).

In this work, kinetic analysis of the data could be best fitted to a model which assumes sequential changes in conformation on binding and release of the metal ions. The results were discussed in relation to the possible role of these conformational changes in the mechanism of catalysis and regulation of CF_1.

Materials and Methods

Enzyme Preparation. CF_1 was isolated from spinach chloroplasts (Binder et al., 1978). Stored CF_1 (Hiller & Carmeli, 1985) was passed through a centrifuged G-50 Sephadex column equilibrated with 40 mM HEPES–NaOH, pH 8, and 1 mM ATP. Following incubation for 1 h, the enzyme was passed twice through a centrifuged G-50 Sephadex column equilibrated with 40 mM HEPES–NaOH, pH 8. ATPase activity was determined (Hiller & Carmeli, 1985) following heat activation (Farron & Racker, 1970). For metal binding studies, the enzyme was concentrated by ultrafiltration to ~50 μM. Protein concentration was determined by UV absorption (Farron & Racker, 1970).

Rapid Kinetic Measurement of Mn^{2+} Binding. Time-dependent changes of the concentration of free Mn^{2+} were monitored by a Varian E-109 EPR spectrometer interfaced with a Nicolet 1280 computer. The absorption of free Mn^{2+} was recorded with the field set at 3419 G, a modulation amplitude of 25, and a microwave power of 10 mW. The free Mn^{2+} gives a sharp absorption spectrum while the CF_1-bound

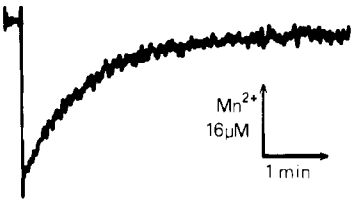

FIGURE 1: Time course of the release of bound Mn^{2+} from CF_1. CF_1, 56 μM, which was preincubated with 0.2 mM $MnCl_2$ was rapidly mixed with an equal volume of 5 mM $MgCl_2$. The change in absorption was monitored by an EPR spectrometer.

Mn^{2+} gives an extremely broad spectrum in the X-band frequency region. A solution of approximately 50 μM CF_1 and 40 mM HEPES–NaOH, pH 8, was mixed in a rapid-mixing device (response time 8 ms) (Cafiso & Hubbell, 1982) with an equal volume of 100 μM $MnCl_2$ (or as indicated) and 40 mM HEPES–NaOH, pH 8. The release of Mn^{2+} was measured by mixing CF_1 preincubated with $MnCl_2$ with an equal volume of 5 mM $MgCl_2$ and monitoring the increase of free $[Mn^{2+}]$ in EPR.

Calculations. For analysis of the data, the model of binding (see Scheme I under Results) was expressed as sets of differential rate equations (see eq 1–3 under Results) interrelated with mass law equations (see eq 4 and 5 under Results). The sets were solved numerically with the DVERK subroutine of the IMSL library based on the Runge–Cutta–Vernier algorithm (Hull et al., 1976). Curve fitting to the experimental data was done by nonlinear regression using the MINITAB statistical package (Ryan & Ryan, 1976). The kinetic model (eq 1–5) was used to best fit the rate constants to the experimental curves by χ^2 minimization with the aid of the CERN MINUIT program (James & Roos, 1975), using the algorithms SIMPLEX (Nelder & Mead, 1965), MIGRAD (Fletcher, 1970), and IMPROVE (Goldstein & Price, 1971). The minimization limit was set to 1% standard deviation. The interdependence of the final parameters gave a rather large error which was especially apparent in the off-rate constants (Tables I and II).

The calculated kinetic parameters (Table I) were used to simulate the binding at equilibrium of Mn^{2+} at concentrations varying from 0 to 5 mM. The calculated binding data were used to construct theoretical Scatchard plots.

Results

Rapid Kinetic Measurements. Measurements of fast binding and release of Mn^{2+} with a time resolution down to 8 ms were obtained by recording of the changes in the concentration of free Mn^{2+} by an EPR spectrometer following rapid mixing. The rate of the release of Mn^{2+} was measured by rapidly mixing $MgCl_2$ with CF_1 to which Mn^{2+} was bound by preincubation with $MnCl_2$. A fast decrease in the concentration of the free Mn^{2+} was a result of the dilution which occurred during the mixing of $MgCl_2$ solution with latent CF_1 preincubated with $MnCl_2$. This downward deflection was followed by a time-resolved release of the cation (Figure 1). The release was due to exchange of bound Mn^{2+} with the EPR-silent Mg^{2+} ions. In the presence of a 33-fold excess of Mg^{2+} to Mn^{2+}, a time course of the release of Mn^{2+} from 1.5 sites was recorded. Calculations indicate that most of the released Mn^{2+} was recorded. The kinetic experiments were conducted at Mn^{2+} concentrations below full saturation because at higher concentrations the small change in concentration of the free ion due to binding gave too large errors. As is expected, the apparent K_d for binding was lower than the average of 14.5 μM (Hiller & Carmeli, 1985) obtained for the three cooperative sites at saturation. Therefore, the

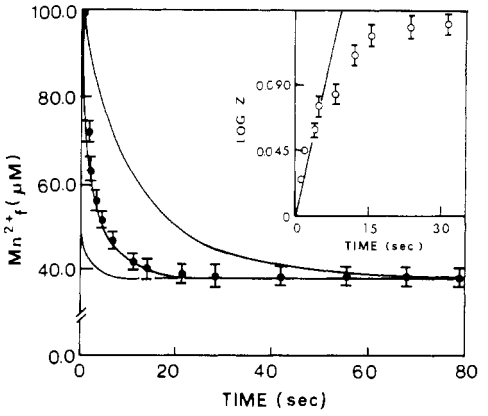

FIGURE 2: Time course of Mn^{2+} binding to CF_1. Latent CF_1, 56 μM, was rapidly mixed with an equal volume of 0.2 mM $MnCl_2$, and the time course of binding was monitored by an EPR spectrometer. The average of five runs (●) was plotted together with the curve best fitted by calculations according to the sequential ordered scheme as indicated under Materials and Methods. A 5-fold increase or decrease in the rate constants obtained from the best fit produced the lines below and above the data, respectively. The insert represents an overall second-order plot of the average of data obtained from 10 runs (○). log Z [$Z = (B_0/A_0)(A_0 - X/B_0 - X)$] was plotted versus time where A_0 and B_0 are the initial concentrations of the two reactants and X is the change in the concentration of one of the reactants, free Mn^{2+}.

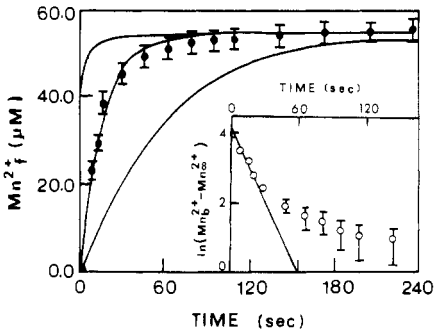

FIGURE 3: Time course of the release of bound Mn^{2+} from CF_1. The average of recorded five runs (●) of the release of the metal from 52 μM latent CF_1 which had been preincubated with 0.124 mM $MnCl_2$ and rapidly mixed with a 33-fold excess of $MgCl_2$, as indicated under Figure 1. Five-fold larger or smaller rate constants than those obtained from the best fit were used for calculation of the curves above and below the data, respectively. The insert represents a ln plot of an average of 10 runs in micromolar of the change in the concentration of bound Mn^{2+} (Mn^{2+}_b) minus the concentration of the bound ion at equilibrium (Mn^{2+}_∞) versus time.

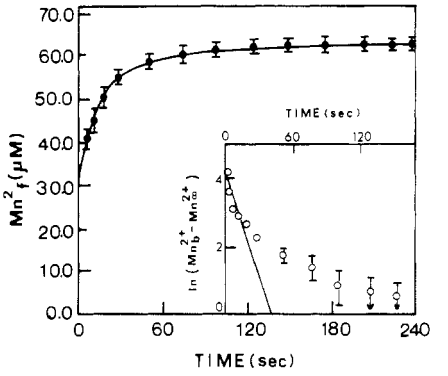

FIGURE 4: Release of Mn^{2+} from heat-activated CF_1. Following heat activation, 50 μM enzyme was preincubated with 0.150 mM $MnCl_2$, and the release of the metal was measured as indicated undr Figure 3. The insert represents a ln plot of the data as indicated under Figure 3. The experimental conditions and the calculation of the fitted curve were as indicated under Materials and Methods.

calculated value of binding to 2.2 sites at the final concentrations of metal and enzyme in the experimental conditions described under Figure 1, that was expected for K_d at saturation conditions, was higher than the measured value. Although the release was a result of exchange between the two cations, it was assumed that the rate-limiting step in this process was the dissociation of the metal which was not greatly affected by the rebinding of another cation under the given conditions. Indeed, similar rates were observed (Hiller & Carmeli, 1988) when the release of enzyme-bound Mn^{2+} was measured by direct chelation to a chromophore in the absence of an exchanging cation.

Binding was measured following the mixing of CF_1 with $MnCl_2$ (trace not shown). Measurements of the amount of bound Mn^{2+} at the end of the run indicated that part of the cation binds faster than the response time of the instrument and therefore was not recorded. Indeed, when heat-activated CF_1 was rapidly mixed with $MnCl_2$, no transient change was recorded. Similar binding capacity was determined for both the latent and the activated CF_1. Therefore, the lack of recorded changes was an indication that the kinetics of binding of Mn^{2+} to the heat-activated CF_1 were faster than 8 ms which was the time resolution of the measuring system. It was also faster than the slow phase but could be similar to the rate of the faster phase of Mn^{2+} binding to the latent enzyme.

The purified CF_1 used in these experiments contains approximately one Mg^{2+} bound per enzyme which is very difficult to exchange or remove (Girault et al., 1982; Hiller & Carmeli, 1985). This site is probably specific for Mg^{2+} and might be the noncatalytic site where MgATP binds extremely tightly (Bruist & Hammes, 1981). This site is also different from the three interacting metal sites to which binding was measured in this work. Almost all the $^{54}Mn^{2+}$ was removed from CF_1, after preincubation with this metal, by passage through two successive Sephadex centrifugation columns (data not shown), a treatment that failed to remove the tightly bound Mg^{2+}.

Kinetic Models for Calculations. Initial attempts to analyze the binding as an overall second-order kinetic process indicated the involvement of multiple rate constants as no single straight line could fit the data (Figures 2 and 5, inserts). More than one rate constant was also observed in the analysis of the release of ions from CF_1 (Figures 3 and 4, inserts) since the data could not fit a single straight line in the log plot (see also Discussion). It was therefore necessary to design a kinetic model for the analysis of the data. It was reasonable to assume that the observed slow rate of Mn^{2+} binding to the latent enzyme and the slower rate of Mn^{2+} release are related to the conformational changes in the enzyme, which caused changes in the binding properties. These could be the changes that induced the cooperative interaction among the three tight Mn^{2+} binding sites in CF_1 (Hiller & Carmeli, 1985). A model by which the data could be explained and analyzed was suggested (Scheme I). The model assumed that the metal-free CF_1 (E) could bind Mn^{2+} (M) to one site, exciting a reversible conformational change (E*M) which was expressed as a decrease in the dissociation constants of the metal binding. The binding and conformational changes were sequentially transmitted through the three binding sites.

Scheme I

$$E + M \underset{k_{-1}}{\overset{k_1}{\rightleftharpoons}} {}^{*}EM + M \underset{k_{-2}}{\overset{k_2}{\rightleftharpoons}} {}^{**}EM_2 + M \underset{k_{-3}}{\overset{k_3}{\rightleftharpoons}} {}^{***}EM_3$$

In Scheme I k_1, k_2, and k_3 and k_{-1}, k_{-2}, and k_{-3} were the respective kinetic on-rate and off-rate constants of the three binding sites. For numerical analysis of the binding parameters, Scheme I was described as three differential equations (eq 1–3) using a modification of the model suggested by Adair

Table I: Rate Constants for Mn^{2+} Binding to CF_1[a]

enzyme	on-rate constants ($\times 10^4$ M^{-1} s^{-1}), $k_1 = k_2 = k_3$	off-rate constants (s^{-1}) $k_{-1} = k_{-2}$	k_{-3}
LCF_1	1.1 ± 0.037	0.69 ± 0.035	0.055 ± 0.003
LCF_1 ADP	0.98 ± 0.12	0.31 ± 0.020	0.033 ± 0.008
HCF_1	4.20 ± 0.92	1.34 ± 0.080	0.160 ± 0.007

[a] The values were obtained for the three cooperatively interacting binding sites from the fit of the experimental data to the theoretical formulation using the ordered sequential model as indicated. L, latent; H, heat-activated; ADP, 1 equiv added per CF_1.

(1925). The differential equations are interdependent through mass law equations (eq 4 and 5). Here, $[M_t]$, $[M]$ and $[E_t]$, $[E]$ are the concentrations of the total and the free metal and enzyme, respectively. Either the binding could start at a defined site on the enzyme and proceed in an ordered fashion to the second and the third sites, or it might randomly start at any site and proceed to the rest.

$$d[EM]/dt = [E][M]k_1 - [EM]k_{-1} - [EM][M]k_2 + [EM_2]k_{-2} \quad (1)$$

$$d[EM_2]/dt = [EM][M]k_2 - [EM_2]k_{-2} - [EM_2][M]k_3 + [EM_3]k_{-3} \quad (2)$$

$$d[EM_3]/dt = [EM_2][M]k_3 - [EM_3]k_{-3} \quad (3)$$

$$[M_t] = [M] + [EM] + 2[EM_2] + 3[EM_3] \quad (4)$$

$$[E_t] = [E] + [EM] + 2[EM_2] + 3[EM_3] \quad (5)$$

Fit of the Kinetic Models to the Data. In an attempt to fit theoretical curves to the data, one to six rate constants were used for the equations of the ordered sequential model of binding. The data could only be fitted with a minimum of three different rate constants. A fit to the data of the binding of Mn^{2+} to latent CF_1 is shown in Figure 2. The three on-rate constants were fitted with a common value while the first two had a common off-rate constant and the third had a different value. The fitted curve deviates only by 1% from the mean of the experimental data, while a 5-fold increase or decrease in the rate constants obtained from the best fit drastically deviated from it (Figure 2, lines below and above the data, respectively). The same model could also be used for the fit of the time course of the release of the metals from the latent enzyme (Figure 3). Visual presentation of the accuracy of the analysis was given by calculation of curves having 5-fold larger or smaller rate constants than those obtained from the best fit. The release was much slower than the binding of metals. Yet it was accelerated when the enzyme was heat-activated. Only the tail end of the release was recorded because the initial phase was faster than the response time of the instrument (Figure 4). As already mentioned, the binding to the heat-activated CF_1 was faster than the response time and much faster than the binding to the latent enzyme.

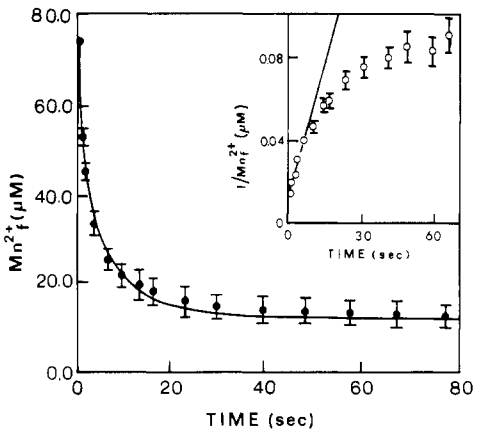

FIGURE 5: Effect of ADP on the binding of Mn^{2+} to CF_1. The kinetics of Mn^{2+} binding to latent CF_1 were measured following the preincubation of 50 μM enzyme with 1 equiv of ADP. The enzyme was rapidly mixed with a solution containing 0.15 mM $MnCl_2$ under experimental conditions as described under Figure 2. The insert represents an overall second-order plot of an average of 10 runs of binding between equal concentrations of the metal and the binding sites ($3/CF_1$). The reciprocal of the change in the concentration of free Mn^{2+} minus the concentration at equilibrium (O) was plotted versus time.

Knowing that nucleotides decrease the dissociation constant of metal binding to CF_1, it was interesting to evaluate their effect on the kinetics of binding. It seems that the rate of binding in the presence of ADP was only slightly slower than the rate in its absence (Figure 5). The change therefore was mostly a result of a slower rate of release (not shown). Under the experimental conditions, most of the ADP was bound to the enzyme as its dissociation constant of 1 μM (Bruist & Hammes, 1981) is much lower than that of the Mn·ADP complex. Therefore, what was measured was the binding to the enzyme and not to the ADP.

Calculated Kinetic Constants. The two most distinguished characteristics of the kinetic behavior of Mn^{2+} binding were the heterogeneity of the various sites and the dramatic change in the calculated rate constants which were caused by heat activation. The off-rate from the third site was 10–20-fold slower than from the other two (Table I). Heat activation of the enzyme caused a 2–4-fold increase in both the on-rate and the off-rate constants, resulting in an overall faster binding to the enzyme. Binding of a single ADP per enzyme caused only a slight decrease in the off-rate constants. The effect of ADP was reminiscence of the slow down caused by this agent in ATP hydrolysis catalyzed by the membrane-bound enzyme (Carmeli & Lifshitz, 1972). Heat activation induced a 2–4-fold increase in all rate constants, but there was no alteration in the heterogeneity of the various sites.

The random sequential model differs from the ordered version only by the inclusion of statistical factors for binding to the various sites. For calculations of the rate constants according to the random model, factors of $^1/_3$, $^1/_2$, and 1 were used for the first, second, and the third sites, respectively (Hopfield et al., 1971). As seen from Table II, a random mechanism required that each of the sites had an on-rate and

Table II: Rate Constants for Mn^{2+} Binding to CF_1[a]

enzyme	on-rate constants ($\times 10^4$ M^{-1} s^{-1}) k_1	k_2	k_3	off-rate constants (s^{-1}) k_{-1}	k_{-2}	k_{-3}
LCF_1	0.37 ± 0.01	0.55 ± 0.02	1.1 ± 0.04	0.69 ± 0.04	0.35 ± 0.02	0.02 ± 0.001
LCF_1 ADP	0.33 ± 0.04	0.49 ± 0.06	0.98 ± 0.1	0.31 ± 0.02	0.15 ± 0.01	0.11 ± 0.03
HCF_1	1.4 ± 0.30	2.1 ± 0.46	4.2 ± 0.92	1.34 ± 0.08	0.67 ± 0.04	0.05 ± 0.02

[a] The values were obtained for the three cooperatively interacting binding sites from fit of the experimental data to the theoretical formulation using the random sequential model. L, latent; H, heat-activated; ADP, 1 equiv added per CF_1.

Table III: Thermodynamic Dissociation Constants of Mn^{2+} Binding to the Three Cooperatively Interacting Sites in CF_1[a]

	dissociation constants (μM)				
	ordered		random		
enzyme	$K_1 = K_2$	K_3	K_1	K_2	K_3
LCF_1	63	5.0	186	64	1.63
LCF_1 ADP	32	3.4	94	31	1.12
HCF_1	32	3.8	96	32	1.16

[a] The values were calculated from the data in Tables I and II for the latent (L) and heat-activated (H) CF_1 by using the ordered and the random sequential models. One equivalent of ADP/CF_1 was added (ADP).

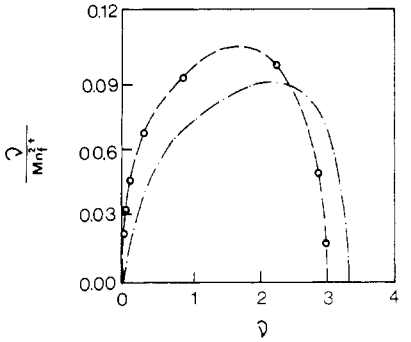

FIGURE 6: Scatchard plots of Mn^{2+} binding to CF_1. The calculated kinetic constants were used for simulation of binding at equilibrium (O—O). The amount of bound ion per CF_1 (ν) is plotted against ν divided by the concentration of free ion (Mn^{2+}_f) at various added concentrations of $MnCl_2$. The data from equilibrium binding studies (–·–) were as previously published by Hiller and Carmeli (1985).

an off-rate constant which differ from those of the other sites.

Dissociation Constants. The thermodynamic dissociation constants (Table III) were essentially a direct resultant of the rate constants. The dissociation constants calculated according to the ordered sequential and the random models differ by factors of 3, 1, and $^1/_3$ for the first, second, and third sites, respectively (Adair, 1925). In the presence of ADP and in heat-treated enzyme, the dissoication constants for the first and the second sites were lower than those for the same sites in the latent CF_1. Yet, under any condition, the third site had 10–100-fold lower dissociation constants than the two other sites. This finding was in agreement with the slower release observed from these sites. The mean of any three dissociation constants calculated according to the two models (data not shown) compared well to the mean dissociation constants for the three sites obtained from calculation with the Scatchard equation (Hiller & Carmeli, 1986).

Theoretical Scatchard Plot. Verification of the involvement of the binding sites in cooperative interactions was afforded by the use of the rate constants for simulation of binding of Mn^{2+} at equilibrium. The calculated amounts of bound and free metal at added concentrations ranging from 0 to 5 mM $MnCl_2$ were used to construct Scatchard plots (Figure 6). The downward concave curve which intercepts at the value of 3 on the x axis represents binding to three strongly cooperative interacting sites. These data resembled the isotherm obtained earlier (Hiller & Carmeli, 1985) from equilibrium binding studies and drawn here for comparison. A slight difference in calculation causes the theoretical curve to originate at a value higher than 0 on the y axis. This was because the value of the binding constant of the first site, before it underwent cooperative interaction, was not subtracted as was done in the calculation of the data obtained from equilibrium binding studies.

Restrictions in the resolution of the measuring system required that the kinetic experiments were conducted in Mn^{2+} concentrations which gave only partial saturation of the three interacting binding sites. Yet the calculated rate constants probably did not differ from those that could be obtained under saturation conditions. This is apparent from the fact that when the calculated rate constants were used to simulate binding at equilibrium, full cooperative interaction was obtained.

Discussion

Conformational Changes. It is widely accepted that conformational changes transmitted through subunit interactions are important in control mechanisms of the F_1-type ATPases. Hackney et al. (1979) further proposed that conformational changes not only are required for regulation but also serve as a mean by which the electrochemical potential of protons is utilized for ATP synthesis by this enzyme. It is, therefore, of interest to study the properties of the cooperative interactions in this enzyme. The kinetics of Mn^{2+} binding served as a probe for the dynamic properties of cooperative interactions among the subunits, the basic premise being that the observed binding rate of the metal is correlated to the rate at which the dissociation constants were altered and the latter being correlated to the rate of the conformational changes.

Models of Cooperativity. Analysis of the binding of Mn^{2+} to CF_1 as an overall second-order kinetic process indicated multiple rate constants (Figures 2 and 5, inserts). The release of the metal was also found to consist of several rate constants (Figures 3 and 4, inserts). In an attempt to quantitate the kinetic and the thermodynamic properties of the binding cations, several kinetic models were used. Neither the kinetic nor the equilibrium binding data could be well fitted to a number of models which did not assume cooperative interactions following the formulation by Segel (1980) (data not shown). Since equilibrium binding studies clearly indicated a strong cooperative interaction among three binding sites on the enzyme, it was reasonable to consider such an interaction in an attempt to fit the kinetic data. Indeed, the data were fitted to models of cooperative binding such as those first proposed by Adair (1925). The analysis followed earlier attempts to study the kinetics of cooperative changes conducted by Eeigen (1967) and Hopfield et al. (1971). The simplest models to which the data could be fitted were the Adair (1925) model and its modified version. The modified version assumed sequential ordered binding and transmission of the cooperative changes which start from a defined site as described in Scheme I. It differed from the original model which assumed that the binding can start at any site and therefore did not have statistical factors of 3, 1, and $^1/_3$ for the thermodynamic dissociation constants of sites 1, 2, and 3, respectively. Otherwise, the two models were mathematically equal.

The third model to which the data could be fitted was the kinetic analysis of Hopfield et al. (1971) based on the theory of Monod et al. (1965). As the data could be fitted to this model, the operation of such a mechanism in the CF_1 could not be excluded. Yet, the mathematical equations of this model employ more constants than the Adair models and therefore could possibly accommodate a wider range of apparent kinetic patterns.

The kinetic analysis was insufficient for determination of a model which best describes the mechanism as the data could be fitted to various models of cooperativity. However, the ordered sequential model seem to be favored because of the transient structural asymmetry in the three β subunits of CF_1, which is expressed in the fact that one of them contains a tightly bound ADP (Abbott et al., 1984), and in their heterogeneous labeling by chemical modification (Zhixiong et al.,

1987). Kinetic analysis of catalytic rates also favors the existence of sequential binding and release of substrates and products at the three active sites, as catalysis proceeds from one active site to another (Stroop & Boyer, 1987).

Relevance to the Kinetics of Regulation and Catalysis. (*A*) *Dissociation Constants.* The thermodynamic dissoication constants of the three interacting sites are in the range of 1–20 μM for both the Mn^{2+} ions (Hiller & Carmeli, 1986; Haddy et al., 1985) and the nucleotides (Bruist & Hammes, 1981). These are believed to represent the dissociation constants of the substrate of ATPase. Although the K_s was not directly measured, it should be similar as the substrate is a complex of metal–nucleotide. Assuming a k_{cat} of 50–400 s^{-1}, the calculated K_m is in the range of 0.1–1 mM as experimentally obtained (Bruist & Hammes, 1981).

It seems apparent from the data that the thermodynamic dissociation constants of the cations and the nucleotides and therefore also that of the substrate did not greatly change when the enzyme was converted from latent to active state and probably stayed the same also during steady-state catalysis. However, the on-rate constants changed dramatically as the enzyme was activated and during catalysis. As discussed earlier, the changes in on-rate constants are suggested to be correlated to alterations in the rates of the conformational changes. Therefore, it is suggested that activation was due to allowance of faster transmission of structural changes required for catalysis among the subunits of the enzyme.

(*B*) *Activation of Catalysis.* A closer comparison between the rates of activation and catalysis and the rate constants of cation binding produced revealing correlations. Although on heat activation of the latent enzyme there was an increase in the rate constants for cation binding, the off-rate constant of the third site remained the slowest and was similar to the apparent rate constant for the acceleration of ATPase activity in an enzyme to which cations have been bound prior to the addition of substrate (Carmeli et al., 1981). It seemed, therefore, that the activation of catalysis in the three sites was correlated to the rate of the structural change which allowed the relase of cation from the third site. Indeed, the rate constant for the release of the tightly bound ADP was also approximately 0.05 s^{-1} under similar conditions (Leckband & Hammes, 1987). This nucleotide was also involved in regulation through binding to one of the active sites. In the absence of bound cation, the rate constants both for acceleration of catalysis (Carmeli et al., 1981) and for the release of the bound ADP (Wu & Boyer, 1986) were 1 s^{-1}. Although not determined, in analogy to the other cases, it was expected that the rate constant for the metal was also similar under these conditions. Indeed, the rate constant both for the acceleration of catalysis and for the release of metal from the active isolated CF_0F_1 was faster than 5 s^{-1} (Hiller and Carmeli, unpublished observation) as it was faster than the response time of the measuring system. The fact that binding of metals and nucleotides induces conformational changes indicated that although the rate of the release of these ligands is dependent on the rate of the structural change, the latter was also affected by the presence of these ligands.

(*C*) *Steady-State Catalysis.* At steady state, the rate of binding and release of transiently tightly bound nucleotides was shown to be compatible with the rate of catalysis (Rosen et al., 1979). As tight binding of nucleotides was probably induced by the same cooperatively transmitted structural changes, it is expected that under steady-state conditions the rate of metal binding was also compatible with the rate of catalysis. Although the rate of metal binding at steady-state catalysis is yet to be measured, previous findings presented here concerning the similarities in the rate constants of nucleotide and metal binding, and the evidence for the presence of nucleotide–metal complex as substrate, support the assumption that the rate of metal binding and release during steady state is also compatible with the rate constants of substrate binding.

Acknowledgments

Part of this work was done by Dr. C. Carmeli during a visit to the laboratory of Dr. P. D. Boyer at the Institute for Molecular Biology at UCLA. We thank Dr. Boyer for collaboration and support and Dr. W. L. Hubbell from the Jules Stein Eye Institute at UCLA for the use of the EPR instrument and for his assistance.

Registry No. ATPase, 9000-83-3; Mn, 7439-96-5; ADP, 58-64-0.

References

Abbott, M. S., Czarnecki, J. J., & Selman, B. R. (1984) *J. Biol. Chem. 259*, 12271–12278.

Adair, G. S. (1925) *J. Biol. Chem. 63*, 529–545.

Bakker-Grunwald, T., & Van Dam, K. (1974) *Biochim. Biophys. Acta 347*, 290–298.

Binder, A., Jagendorf, A. T., & Ngo, E. (1978) *J. Biol. Chem. 253*, 3094–3100.

Bruist, M. F., & Hammes, G. G. (1981) *Biochemistry 20*, 6298–6305.

Bruist, M. F., & Hammes, G. G. (1982) *Biochemistry 21*, 3370–3377.

Cafiso, D. S., & Hubbell, W. L. (1982) *Biophys. J. 39*, 263–272.

Carmeli, C., & Lifshitz, Y. (1972) *Biochim. Biophys. Acta 267*, 86–97.

Carmeli, C., Lifshitz, Y., & Gutman, M. (1981) *Biochemistry 20*, 3940–3944.

Carmeli, C., Huang, J. Y., Mills, D. M., Jagendorf, A. T., & Lewis, A. (1986) *J. Biol. Chem. 261*, 16969–16975.

Carmeli, C., Hiller, R., & Boyer, P. D. (1987) in *Progress in Photosynthesis Research* (Biggins, J., Ed.) Vol. III, pp 123–126, Martinus Nijhoff, Dordrecht, The Netherlands.

Cross, R. L. (1981) *Annu. Rev. Biochem. 50*, 681–714.

Eiegen, M. (1967) *Nobel Symp. No. 5*, 333–350.

Farron, F., & Racker, E. (1970) *Biochemistry 9*, 3829–3834.

Fletcher, R. (1970) *Comput. J. 13*, 317–320.

Girault, G., Galmiche, J. M., Lemaire, C., & Stulzafz, O. (1982) *Eur. J. Biochem. 128*, 405–411.

Goldstein, A. A., & Price, J. F. (1971) *Math. Comput. 25*, 569–572.

Hackney, D. P., Rosen, G., & Boyer, P. D. (1979) *Proc. Natl. Acad. Sci. U.S.A. 76*, 3646–3650.

Haddy, A. E., Frash, W. D., & Sharp, R. R. (1985) *Biochemistry 24*, 7926–7930.

Hillel, R., Jagendorf, A. T., & Carmeli, C. (1984) in *Advances in photosynthesis research* (Sybesma, C., Ed.) Vol. 2. pp 511–517, Martinus Nijhoff/Dr. Junk Publishers, The Hague, The Netherlands.

Hiller, R., & Carmeli, C. (1985) *J. Biol. Chem. 260*, 1614–1617.

Hiller, R., & Carmeli, C. (1988) in *Ion Pumps; Structure, Function and Regulation* (Stein, W. D., Ed.) pp 307–314, Alan R. Liss, New York.

Hopfield, J. J., Shulman, R. G., & Ogawa, S. (1971) *J. Mol. Biol. 61*, 425–443.

Hull, T. E., Enright, W. H., & Jackson, K. R. (1976) *User's Guide for DVERK—A Subroutine for Solving Non-Stiff ODE's*, University of Toronto Press, Toronto.

James, F., & Roos, M. (1975) *Comput. Phys. Commun. 10*, 343-367.
Junesch, U., & Graberr, P. (1987) *Biochim. Biophys. Acta 893*, 275-288.
Leckband, D., & Hammes, G. G. (1987) *Biochemistry 26*, 2306-2312.
McCarty, R. E., & Carmeli, C. (1982) in *Photosynthesis: Energy conversion by Plants and Bacteria* (Govindjee, Ed.) Vol. 1, pp 647-695, Academic Press, New York.
Monod, J., Wyman, J., & Changeux, J. P. (1965) *J. Mol. Biol. 12*, 88-118.
Morony, J. V., Lopreti, L., McEwen, B. F., McCarty, R. E., & Hammes, G. G. (1983) *FEBS Lett. 158*, 58-62.
Nelder, J. A., & Mead, R. (1965) *Comput. J. 7*, 308-312.
Rosen, G., Gresser, M., Vinkler, C., & Boyer, P. D. (1979) *J. Biol. Chem. 254*, 10654-10661.
Ryan, J., & Ryan, D. (1976) *MINITAB Student Handbook*, Duxbury Press, New York.
Segel, L. A. (1980) *Mathematical Models in Molecular and Cellular Biology*, pp 39-55, Cambridge University Press, Cambridge.
Stroop, S. D., Boyer, P. D. (1987) *Biochemistry 26*, 1479-1484.
Strotmann, H., & Bickel-Sandkotter, S. (1977) *Biochim. Biophys. Acta 400*, 126-135.
Takabe, T., Debenedetti, E., & Jagendorf, A. T. (1982) *Biochim. Biophys. Acta 682*, 11-20.
Wu, D., & Boyer, P. D. (1986) *Biochemistry 25*, 3390-3396.
Zhixiong, X., Jun-Mei, Z., Melese, T., Cross, R., & Boyer, P. D. (1987) *Biochemistry 26*, 3749-3753.

^1H and ^{31}P Nuclear Magnetic Resonance and Kinetic Studies of the Active Site Structure of Chloroplast CF_1 ATP Synthase†

Cathy C. Devlin and Charles M. Grisham*
Department of Chemistry, University of Virginia, Charlottesville, Virginia 22901
Received September 13, 1989; Revised Manuscript Received February 5, 1990

ABSTRACT: The interaction of nucleotides and nucleotide analogues and their metal complexes with Mn^{2+} bound to both the latent and dithiothreitol-activated CF_1 ATP synthase has been examined by means of steady-state kinetics, water proton relaxation rate (PRR) measurements, and ^1H and ^{31}P nuclear relaxation measurements. Titration of both the latent and activated Mn^{2+}-CF_1 complexes with ATP, ADP, P_i, $Co(NH_3)_4ATP$, $Co(NH_3)_4ADP$, and $Co(NH_3)_4AMPPCP$ leads to increases in the water relaxation enhancement, consistent with enhanced metal binding and a high ternary complex enhancement. Steady-state kinetic studies are consistent with competitive inhibition of CF_1 by $Co(NH_3)_4AMPPCP$ with respect to CaATP. The data are consistent with a K_i for $Co(NH_3)_4AMPPCP$ of 650 μM, in good agreement with a previous K_i of 724 μM for $Cr(H_2O)_4ATP$ [Frasch, W., & Selman, B. (1982) *Biochemistry 21*, 3636-3643], and a best fit K_D of 209 μM from the water PRR measurements. ^1H and ^{31}P nuclear relaxation measurements in solutions of CF_1 and $Co(NH_3)_4AMPPCP$ were used to determine the conformation of the bound substrate analogue and the arrangement with respect to this structure of high- and low-affinity sites for Mn^{2+}. The bound nucleotide analogue adopts a bent conformation, with the low-affinity Mn^{2+} site situated between the adenine and triphosphate moieties and the high-affinity metal site located on the far side of the triphosphate chain. The low-affinity metal forms a distorted inner-sphere complex with the β-P and γ-P of the substrate. The distances from Mn^{2+} to the triphosphate chain are too large for first coordination sphere complexes but are appropriate for second-sphere complexes involving, for example, intervening hydrogen-bonded water molecules or residues from the protein.

Chloroplast coupling factor 1, or CF_1 ATPase,[1] is a latent, soluble membrane protein that couples the synthesis of ATP to proton transport across the thylakoid membranes of green plants. The enzyme has a molecular weight of approximately 400 000, and it exists as an aggregate of five distinct subunits with a stoichiometry of $\alpha_3\beta_3\gamma\delta\epsilon$. Nucleotide binding to the ATPase has been extensively studied by Hammes et al. (Carlier & Hammes, 1979; Bruist & Hammes, 1981; Leckband & Hammes, 1987) while metal binding to the enzyme has been characterized by a number of other researchers (Hochman & Carmeli, 1981; Hiller & Carmeli, 1985; Haddy et al., 1985). The preponderance of the data in these works is consistent with the existence of three nucleotide sites, one of which is believed to be a regulatory ADP binding site, the second of which is believed to bind MgATP with a dissociation half-time on the order of days, and the third of which is believed to be the catalytic site for ADP/ATP turnover. The metal binding studies are consistent with one to three tight,

†Supported by grants from the National Institutes of Health (AM19419), the Muscular Dystrophy Association of America, and the National Science Foundation. The NMR instrumentation used in these studies was provided by grants from the National Science Foundation and the University of Virginia.
* To whom correspondence should be addressed.

[1] Abbreviations: CF_1, chloroplast coupling factor 1; Tricine, *N*-[tris(hydroxymethyl)methyl]glycine; DTT, 1,4-dithio-L-threitol; AMPPCP, adenosine 5'-(β,γ-methylenetriphosphate); CoADP, β,γ-bidentate $Co(NH_3)_4ADP$; CoATP, β,γ-bidentate $Co(NH_3)_4ATP$; Tris, tris(hydroxymethyl)aminomethane; CoAMPPCP, β,γ-bidentate $Co(NH_3)_4AMPPCP$; NMR, nuclear magnetic resonance; EPR, electron paramagnetic resonance; H_{pcp}, protons of the CH_2 group bridging the β- and γ-P of CoAMPPCP.

0006-2960/90/0429-6192$02.50/0